Plant Physiol. (1984) 74, 721–726
0032-0889/84/74/0721/06/$0.100/0

Uronide Deposition Rates in the Primary Root of *Zea mays*[1]

Received for publication May 17, 1983 and in revised form October 17, 1983

WENDY KUHN SILK, ROBERT C. WALKER, AND JOHN LABAVITCH*
Plant Physiology Group, University of California, Davis, California 95616

ABSTRACT

The spatial distribution of the rate of deposition of uronic acids in the elongation zone of *Zea mays* L. Crow WF9 × Mo 17 was determined using the continuity equation with experimentally determined values for uronide density and growth velocity. In spatial terms, the uronide deposition rate has a maximum of 0.4 micrograms per millimeter per hour at $s = 3.5$ mm (*i.e.*, at the location 3.5 mm from the root tip) and decreases to 0.1 mg mm^{-1} h^{-1} by $s = 10$ mm. In terms of a material tissue element, a tissue segment located initially from $s = 2.0$ to $s = 2.1$ mm has 0.14 μg of uronic acids and increases in both length and uronic acid content until it is 0.9 mm long and has 0.7 μg of uronide when its center is at $s = 10$ mm. Simulations of radioactive labeling experiments show that 15 min is the appropriate time scale for pulse determinations of deposition rate profiles in a rapidly growing corn root.

Uronic acids, which are components of the primary cell wall, comprise more than 1% of the total dry weight of the growing region of the corn root. The deposition of uronides occurs as the root cells are expanding and being displaced away from the root tip during growth. Thus, to calculate the local net deposition rates, it is necessary to collect data on the spatial distribution of both growth velocity and concentration of uronides (6, 13–15). The continuity equation of classical fluid dynamics implies that, in quantitative terms,

$$D = \frac{\partial \rho}{\partial t} + \nabla \cdot (\rho v) \quad (1)$$

where D is the local deposition rate, ρ is density (concentration) of the substance of interest, t is time, and v is the growth velocity vector. In the case of a cylindrical, growing organ, equation (1) can be simplified and expanded to

$$D = \frac{\partial \rho}{\partial t} + v\frac{\partial \rho}{\partial s} + \rho\frac{\partial v}{\partial s} \quad (2)$$

where ρ is density (*e.g.*, μg of uronides per millimeter of root length) and s is distance, best measured as millimeters from the root tip (3, 5). On the right side of equation (2), the first term represents the time rate of change of uronide density at a particular spatial location (*e.g.*, 4 mm from the tip). It is termed the local rate of change of uronide density. The second term, $v\,\partial\rho/\partial s$, is the product of growth velocity and spatial gradient in uronide density. It is termed the "convective rate of change," since it represents change due to movement of cells away from the tip. It may be thought of as the component necessary to maintain the spatial gradient in concentration. The sum of the local and convective rates of change equals the "material derivative of uronide density," *i.e.*, the time rate of change of uronide concentration in a material element, such as an infinitesimal tissue segment. The last term in equation (2), $\rho\,\partial v/\rho s$, is the product of strain rate (relative elemental growth rate [2, 3] and uronide density and, as the "stretch component," represents the deposition rate necessary to maintain uronide density in the face of tissue expansion. In the more general case of a radially symmetrical organ, equation (2) may be used as described, but results represent deposition rate per unit length of tissue (see "Appendix"). Determination of the amount of deposition associated with an increase in radius and/or a true increase in volumetric concentration would require a two-dimensional treatment.

Equation (2) suggests measurements to calculate the deposition rates of uronides in growing organs. The primary root of corn, *Zea mays* L., provides an excellent subject for these calculations. Much is known of its distribution of growth rates (3, 4), and comparison can be made to patterns of uronide deposition found with radioactive labeling methods (10, 12). The growing region of the root extends about 1 cm behind the root tip (3) and the diameter is on the order of 1 mm. Below are shown the measurements of the spatial distributions of uronide density and growth velocity (and gradients of density and velocity), and the use of these values to compute the spatial distribution of uronide deposition rates in the longitudinally expanding region of the corn root.

MATERIALS AND METHODS

Plant Material and Growth Conditions. Corn seed (*Zea mays* L., Crow WF9 × Mo 17) were surface sterilized for 10 min in 5.25% hypochlorite and sown in "growth medium" which was vermiculite moistened with 10^{-4} M $CaCl_2$. After approximately 30 h in darkness at 29°C, uniform seedlings with primary roots 3 to 5 mm in length were selected and transferred to growth medium in Plexiglas boxes, built so that the front face slanted 7° from the vertical to allow observation and photography as roots grew along the slanted face. The roots were kept in darkness except for periodic exposure to dim light during inspection, marking, and photography. Roots which had achieved 5 cm length during 18-h incubation were removed for uronic acid analysis or marking and subsequent growth analysis.

Growth Analysis. The apical 15 mm of selected roots were marked with India ink applied with a glass capillary or a steel marking implement scribed to produce marks at 0.5 mm increments. After marking, each root was returned to the growth box and allowed to grow undisturbed for 1 h. Photographs were then taken at five 20-min intervals using an Olympus OM2 camera fitted with macrolens and T32 automated flash triggered by an automatic timer system. The flash was fitted with a combination of colored Plexiglas and cellulose acetate filters to provide a green "safe flash." Photographic prints were made to enlarge the root image 15- to 20-fold. Because the ink dots were deformed during the expansion, the apical or basal edge of an ink dot was used to

[1] Supported by National Science Foundation Grants PCM 78-23710 and PCM 81-00296 to W. K. S. and T. C. Hsiao.

identify a mark on the series of five prints. A Tektronix 4956 Graphics Tablet was used to measure distance of each mark from the root tip. Growth data were analyzed by methods suggested by Erickson (2). At the midpoint of the 100-min time interval, the velocity of displacement of the marks, v, was estimated with the quadratic differentiation formula on positions from five consecutive photographs. Strain rates, $\partial v/\partial s$, were calculated with the five-point quadratic differentiation formula applied to values of velocity interpolated to equally spaced positions using Aitken's interpolation formula (2). Both velocity of displacement and strain rate were used in calculations of uronide deposition rate. Calculations of length and uronide content of a small, growing tissue segment required computer assisted numerical integrations. Cubic splines were used to interpolate the velocity profile to 120 positions spaced 0.1 mm apart. Using the notation proposed by Gandar (7) we can express segment length, L, of the tissue found initially between $s = 2.0$ and 2.1 mm:

$$L = x(2.1, t) - x(2.0, t)$$

where $x(2.1, t)$ represents the current position of the particle found initially at 2.1 mm, and $x(2.0, t)$ represents the current position of the particle found initially at 2.0 mm, and positions are calculated from, *e.g.*,

$$x(2.1, t) = 2.1 + \int_{t_o}^{t} V(2.1, t)\, dt$$

where $V(2.1, t)$ is the current velocity of the particle found initially at $s = 2.1$ mm.

Similarly, segment uronide content was computed from:

$$\text{Uronide} = \rho(2.05, 0)\, \Delta s = \int_{A}^{B} \int_{t_o}^{t} D(2.05, t)\, \text{dt ds}$$

where the apical end of the segment, A, equals $x(2.0, t)$, the basal end of the segment, B, equals $x(2.1, t)$, and D is the deposition rate associated with the current position of the segment.

All figures show position at midpoint of the segment, *i.e.*, 1/2 ($x[2.1, t] + x[2.0, t]$).

Uronic Acid Determination. Roots were rinsed briefly in ice cold, distilled H_2O and excised from the seed. Root caps were removed, and batches of 8 to 10 roots were arranged in a styrofoam jig with their tips together. A series of 12 1-mm sections was cut with an American Optical Model 900 microtome. The sections were collected by position and held on ice until 30 or more had been accumulated. They were then frozen and assayed for uronic acid content within 30 d. For each position, all subsequent procedures were performed in a single test tube without transfers of tissue to maximize recovery, since average sample size was less than 1 mg. Sections were ground in a few drops of ice cold, 80% ethanol and washed five times with 5-ml cold, 80% ethanol. The resulting crude wall preparation was assayed spectrophotometrically for uronic acid content as described by Ahmed and Labavitch (1). Data for uronide content of segments at each position along the root are based upon assays of at least five sets of 10 tissue segments per position. To provide a plot of ρ *versus* s with s resolved in 0.5 mm, two sets of data were combined. For one set, data were obtained between millimeter marks and assigned to the segment midpoint (*e.g.*, $s = 2.5$ mm). For the other, data were obtained for millimeter segments beginning 0.5 mm from the tip and assigned to the millimeter mark (*e.g.*, $s = 3.0$ mm). The term $\partial\rho/\partial s$ was obtained with the five-point quadratic differentiation formula (2) applied to the ρ values, which were first smoothed with the five-point smoothing formula (2).

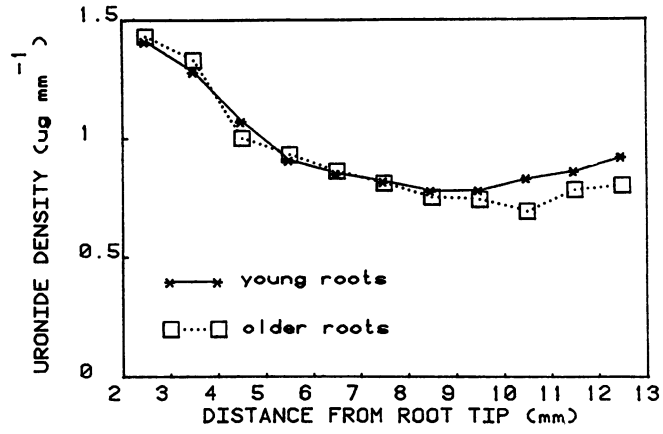

FIG. 1. Uronic acid density (μg mm^{-1} of root length) as a function of position in young, short roots, 3 to 7 cm long (*) and roots 15 h older, 8 to 10 cm long (□).

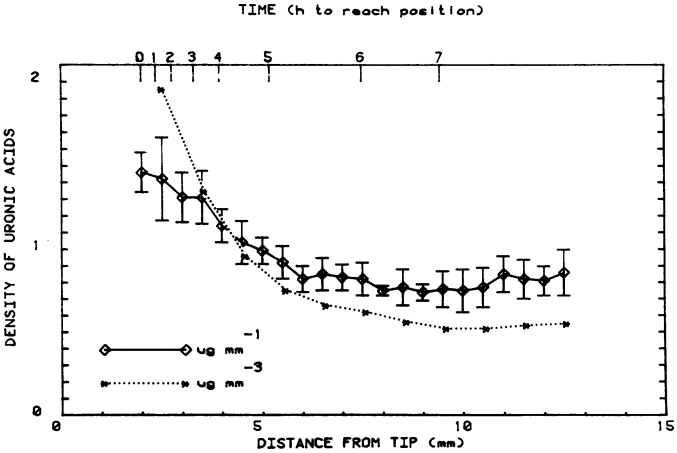

FIG. 2. Uronic acid density (μg mm^{-1} of root length) plotted against distance from the root tip (bottom abscissa). Bars indicate SD for each sample. For an element originally at 2 mm, the position reached after 1, 2, ... 7 h is shown on upper abscissa.

Table I. *Uronic Acid Content of Walls Isolated from 4-mm Segments Cut from Corn Roots*

A sample of 39 roots was cut into 3 lots of segments. Cell wall fraction from these segments were prepared as described in "Materials and Methods."

Segment Location (Relative to Root Tip)	Cell Wall Dry Wt/4-mm Segment	Galacturonic Acid Content/4-mm Segment	Relative Wall Uronide Content
mm	*μg*	*μg eq*	%
0–4	154	4.6	3.0
4–8	108	2.9	2.7
8–12	72	1.9	2.6

RESULTS AND DISCUSSION

Uronide Density. To a first approximation, the distribution of uronide density is steady, *i.e.*, invariant with time, as revealed in preliminary experiments (Fig. 1). Roots approximately 4.5 cm long had a pattern of uronide density similar to that found in roots 9 cm long, even though the longer roots were 15 h older and would have experienced the displacement of several sets of cells. Per millimeter of root length, the uronide content decreases

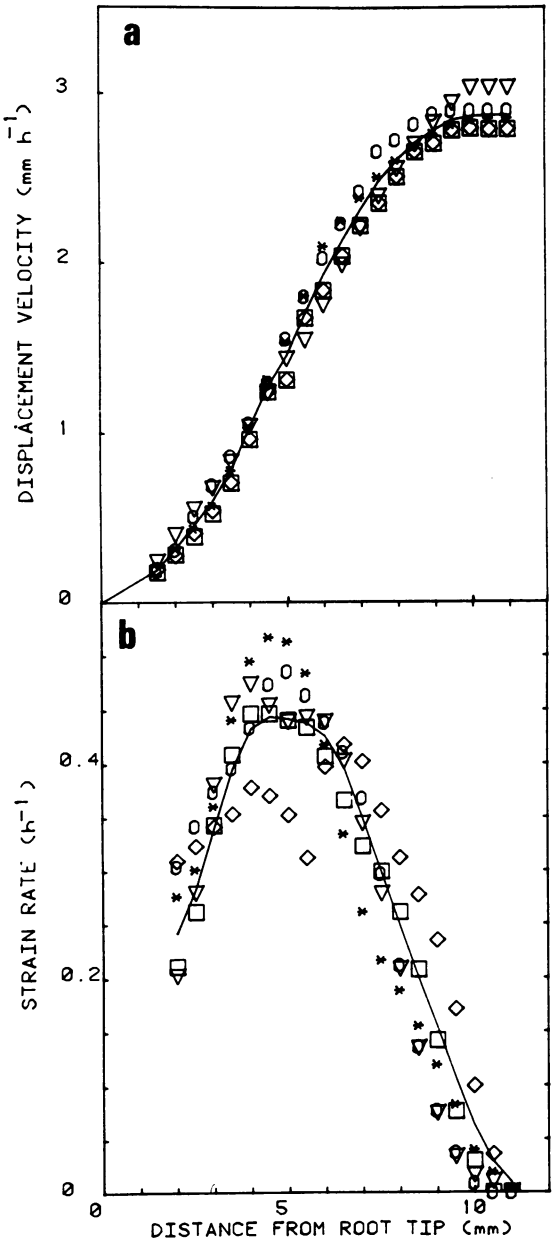

FIG. 3. Growth analysis. Each of five symbols represents values from one root; (——), average value. (a) Rate of displacement of marks from the root tip is plotted against mark position. (b) Derivative of graph in "a" with respect to position gives the strain rate distribution.

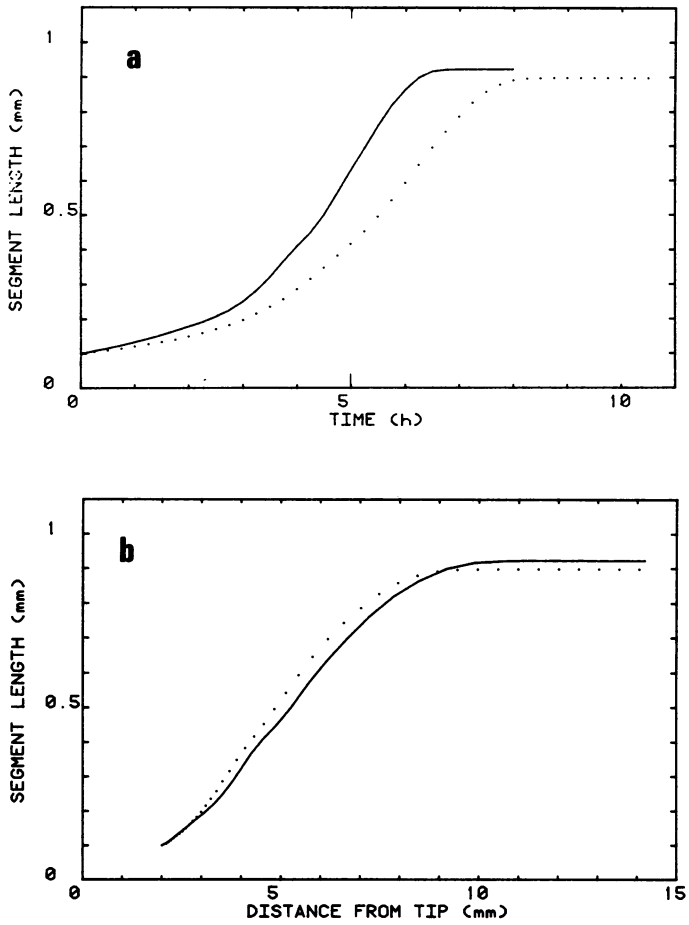

FIG. 4. Growth of a tissue element, initially 0.1 mm long and extending from 2.0 to 2.1 mm, as it is displaced through the growth zone in a rapidly growing root (——) and a more slowly growing root (····). Figures are produced from a numerical integration using the data of Figure 3 and Table I of Reference 4. a, Length of tissue segment plotted against time. b, Length of tissue segment plotted against distance from the root tip.

from 1.45 μg in segments 2 mm from the tip to approximately 0.82 μg found from 6 mm to the base of the growth zone (Fig. 2).

This corresponds to a uronide concentration of 0.012 μg μg^{-1} total dry weight in root tissue located at 2 mm, and of 0.014 μg μg^{-1} dry weight in the tissue located distal to 6 mm. Thus the corn root is very low in uronide content compared to etiolated bean hypocotyls, for which uronic acids have been reported to be 20% of dry weight (16). This substantiates the results of Roberts (Ph.D. Thesis) who found the uronide content of the walls of the corn root very low compared to other tissue, such as cambial tissue. Expressed per unit tissue volume, uronide concentration falls from 1.97 μg mm^{-3} at $s = 2.5$ to 0.53 μg mm^{-3} at $s = 10.5$ mm (Fig. 2).

The decline in uronic acid density with developmental stage (as represented by position in Figs. 1 and 2) could be brought about by the dilution produced by water uptake associated with growth (*e.g.*, fewer crosswalls per millimeter and thinner longitudinal walls) and/or by changes in wall composition. Wall analysis (Table I) suggests (statistical significance not proven) that both processes contribute to the negative convective change, since uronic acids fall from 3.0% to 2.7% of total wall carbohydrate between the first 4-mm and the second 4-mm segments. A tissue age-dependent decline in relative uronide cell wall content has also been described for shoots (9, 16).

Growth analysis, described below, reveals that a tissue element initially at 2 mm, where its uronide density is 1.45 μg mm^{-1} was displaced to the base of the growth zone in a little less than 7 h (Fig. 2).

Growth Velocity and Strain Rate. Root elements accelerate to a constant velocity of displacement from the root tip (Fig. 3a). An element located at 1.5 mm is moving from the tip at 0.19 mm h^{-1}, while at 10.5 mm an element has reached a velocity of almost 2.8 mm h^{-1}. The latter value equals the rate at which the root tip grows down from the soil surface. Displacement of a cellular element is caused by stretching of the cells closer to the tip. Under our experimental conditions the strain rate (relative elemental growth rate [3, 4]) exhibits a broad maximum between 3.0 and 7.0 mm with a peak of 0.45 h^{-1} at 4.5 mm (Fig. 3b). A cell stops stretching (*i.e.*, the strain rate falls to zero) by the time

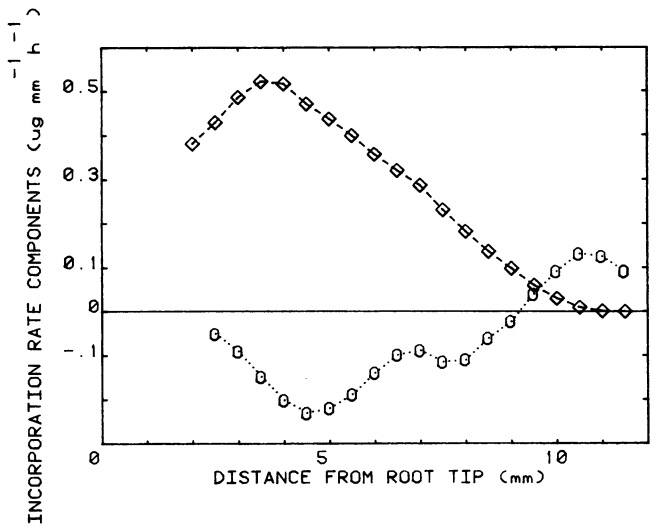

FIG. 5. Components of equation (2): Stretch component (◇); convective rate of change (O).

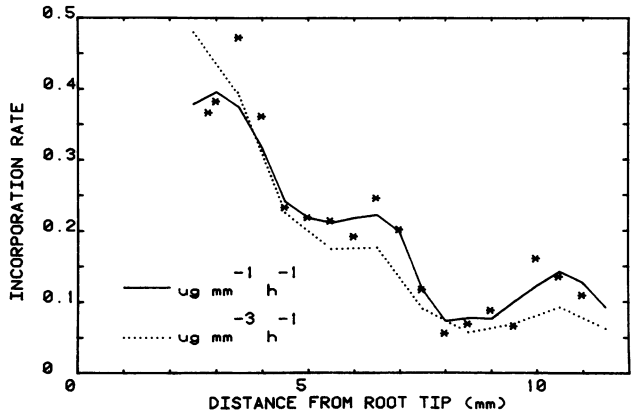

FIG. 6. Uronide deposition rates from Figure 5. Net local deposition rates calculated per unit root length ([*], ——). Asterisks indicate no smoothing of ρ (s); solid line is from smoothed data. Calculated per unit tissue volume (· · · ·).

the cell has been displaced 11 mm from the tip.

It is interesting to compare the strain rate distribution obtained under our conditions with that reported (3, 4) for a corn root growing more slowly (2.0 mm h^{-1}) at a lower temperature (25°C). The growing region is not substantially larger when such a root grows more rapidly at an elevated temperature. At each spatial location the tissue is stretching more rapidly to produce the larger growth velocity of the organ. Theoretically, if the proportionality factor for strain rate increase is the same at each position in the growing zone (*e.g.*, if the strain rate is everywhere twice as great in a faster growing root), a tissue element located at a particular position in the slowly growing root will have experienced the same amount of elongation as an element at the same position in the more rapidly growing root. This is because if the cells elongate more rapidly, they are also displaced more rapidly from each position. This situation is almost true for the corn roots growing at 25°C compared to 29°C (Fig. 4, a and b). For example, a tissue segment extending at 0 time from 2 to 2.1 mm will be 0.42 mm long after 5 h growth at 25°C and 0.63 mm long after 5 h growth at 30°C (Fig. 4a). However, the same tissue elements are each approximately 0.43 mm long when they are centered 4.5 mm from the root tip, regardless of the length of time required to reach the 4.5 mm position (Fig. 4b).

Rates of Uronide Deposition. Information from Figures 1, 2, and 3 was used to evaluate uronide deposition rates in terms of equation (2) (Figs. 5 and 6). Figure 1 implies that the local rate of change, $\partial\rho/\partial t$, is negligible. The most important term numerically is the stretch rate term, $\rho\partial v/\partial s$, which is as high as 0.52 μg mm^{-1} h^{-1} at 3.5 mm and declines to zero at the base of the growth zone (Fig. 5, ◇). Since uronide density declines with distance from the root tip (Fig. 2), the convective rate of change, $v\ \partial\rho/\partial s$ is negative; this means that tissue elements decline in

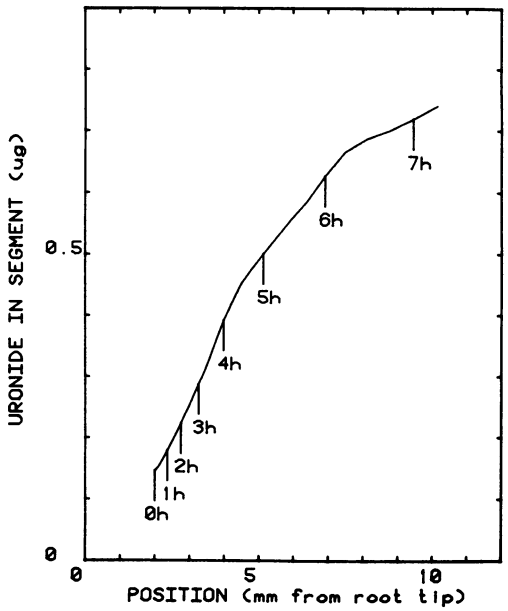

FIG. 7. Uronic acid content of a tissue segment located originally between 2.0 and 2.1 mm as the segment is displaced through the growth zone. Time (h) at which the center of the segment reaches various positions is shown by vertical lines. This figure was produced by a numerical integration using values from Figures 3 and 6.

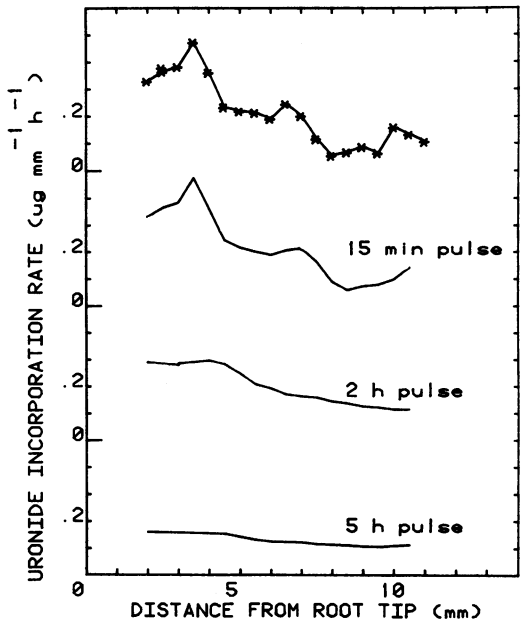

FIG. 8. Computer simulation of results of radioactive labeling experiments. The deposition rate profile of Figures 5 (*) and the growth velocity profile of Figure 3 are assumed. Simulation gives the apparent deposition rate (μg mm^{-1} h^{-1}) which would be found in the absence of labeling artifacts. Curves which would be obtained after 15-min, 2-h, and 5-h pulses are displaced 0.5 units vertically for clarity.

uronide concentration as they are displaced back from the tip. The convective rate of change, which is smaller in magnitude than the stretch rate term, is especially important in the region between 3.5 and 6.5 mm where it ranges from −0.15 to −0.24 $\mu g\ mm^{-1}\ h^{-1}$ (Fig. 5, O). The sum of the stretch rate and convective rate terms is the net local deposition rate (Fig. 6). Uronide deposition occurs throughout the growth zone, with a maximum deposition rate of approximately 0.4 $\mu g\ mm^{-1}\ h^{-1}$ at 3 mm from the tip. Deposition rate falls to 0.1 $\mu m\ mm^{-1}\ h^{-1}$ at $s = 7.5$ mm. In volumetric terms, this corresponds to deposition rates of 0.5 $\mu g\ mm^{-3}\ h^{-1}$ at $s = 2.5$ mm and 0.1 $\mu m\ mm^{-3}\ h^{-1}$ at $s = 7.5$ mm (Fig. 6). (Uronide density increases again behind the elongation zone [not shown]. This implies a rise in uronide deposition rate in more basal regions where stretch does not occur; here we have restricted our discussion to the elongation zone.)

Inspection of Figures 2 and 4 confirms the assertion that uronide deposition occurs throughout the growth zone. The density of uronide decreases to half its original value during the period that the tissue element expands about 9-fold. Thus, a tissue element must accumulate more than four times the amount of uronide which it contained at 2 mm during its displacement through the growth zone. This observation is related to another way to specify uronide content, the Lagrangian specification (7, 14). Uronide deposition rate is shown in Figure 6 as a function of position, and this information can be correlated to other developmental variables (evaluated as functions of position) to infer causal mechanisms for growth physiology. It is also of interest to determine the uronide content of a particular material element, such as a group of cells, as this bit of tissue is displaced through the growth zone (Fig. 7). The cells originally located between 2.0 and 2.1 mm experience both stretch and displacement. Their uronide content increases from 0.14 to 0.8 μg when the center of the segment has been displaced to 10.7 mm.

Comparison with Radioactive Labeling Experiments. The deposition rates found here by evaluating the terms of equation (2) should be obtainable by radioactive labeling methods. It is instructive to compare the results of Figure 6 with those obtained by Roberts and Butt who applied a labeled uronic acid precursor, D-[6-^{14}C]glucuronate, to corn roots and obtained the incorporation rate profile by autoradiography (12) and by isotope counting (10). Our experiments are not strictly comparable, since corn used by Roberts and Butt was of a different strain, the growing region was excised from the seedling before incubation, and incubation was at a lower temperature (25°C) so that growth was much slower. Nevertheless, by a fortuitous coincidence, total growth during the period of incubation in radioactive label was similar to that which occurred between three successive photographs in our experiments. Thus, we would hope that the incorporation patterns might prove similar with the different methods. Roberts and Butt found significant differences in incorporation pattern between cell types, with more deposition in outer cortical cells than in cells of the pith and central stele. Their total incorporation rate profile is quite similar to that of the unsmoothed data of Figure 6 here: the radioactive methods show a peak at $s = 3.5$ mm, representing 25% of the total uronide deposition rate, and a decline with distance until the deposition rate is 5% of the total at $s = 8.5$ mm (6). By comparison, the data of our Figure 6 would show a peak of 23% total deposition rate at $s = 3.5$ mm falling to 5% of the total by $s = 8.5$ mm. It is not meaningful to compare the absolute values for deposition rate because the radioactive uronides were supplied exogenously, while the rates reported here represent the deposition of endogenous substrate.

In evaluating discrepancies between the method of this paper and the labeling experiments, one confronts the difficulty that the radioactive labeling experiment is not instantaneous. Some time is required for penetration of label into the tissue, and in this time period the cells initially at one location will be displaced to another. For instance, under our growth conditions a cell located initially at 4 mm will, 1 h later, be located at 5.2 mm, where the incorporation rate is quite different. As the incubation period increases, the amount of label found at a location is less likely to be an accurate representation of the local deposition rate; the cells at a given location, having arrived from progressively more apical sites, will present an integration of the incorporation rates associated with the different positions traversed en route. It is pertinent to ask over what duration of incubation in radioactive label one can hope to find an accurate picture of the incorporation rate profile. The data of Figures 6 and 3a can be used with the computer integration data from Figure 7 to answer this question (Fig. 8). For a root growing 2.8 mm h^{-1}, a 15-min pulse will reveal the deposition rate assumed. A 30-min pulse (not shown) also gives a reasonable profile, especially in the first half of the growth zone. By 2 h, however, the important characteristics of the deposition rate profile are lost: the peak at 3 mm is not readily observable, and the low values at the basal end of the growth zones are shown as erroneously large. After 5 h incubation in radioactive label the deposition rate profiles appears to be almost flat. Thus, the labeling period for roots growing 2.8 mm h^{-1} should be on the order of 15 min. This is not surprising because the time interval for accurate strain rate analysis is also 15 min. In both sorts of experiments, it is important that the cells at a particular location remain near the attributed sites during the time interval for the observation of change (5, 8). In light of the observation by Roberts and Butt (10) that 3 to 6 h are required for good penetration of polysaccharide precursor into the corn root, it can be concluded that it is not possible to obtain incorporation rate profiles with radioactive label supplied to rapidly growing roots.

The method used here avoids the difficulty with a noninstaneous labeling period but presents statistical difficulties of its own as a result of the computational methods. Numerical differentation does not smooth out errors and gives answers which depend on the distance over which the local approximating functions are fit. Growth analysis results depend on the time scale of the observation period, although one can choose a sufficiently short time interval by repeatedly halving the time between successive photographs until the measured strain rates no longer change with the time interval of the observations (5). With all calculations for material derivatives, one is confronted by the fact that growth velocity increases with distance from the tip so that the effect of a spatial oscillation on the material derivative becomes amplified. Thus, a change of 10% (this is statistically insignificant in the uronide data) between 9.5 and 10 mm will produce a convective rate of change 15 times as great as the same change between 1.5 and 2 mm. If the oscillations are real, then the difference in the effect on the material derivative is real; but where there is experimental error, it will be amplified with distance from the root tip. For this reason, the more apical parts of the deposition rate profile of Figure 6 are probably more accurate than the basal region. Thus, the small peak at 11 mm may be spurious.

Comparison with Other Processes in the Growth Zone. The uronide deposition rate distribution of Figure 6 can be compared with the spatial distribution of several other production rates in the growing zone. In a corn root growing at 25°C the rate of cell production is maximum, about 15,000 cells $mm^{-1}\ h^{-1}$ at 1.5 mm and drops to zero by 3 mm (6). The rate of protein production appears to parallel the rate of cell production, with a maximum of about 1.5 $\mu g\ mm^{-1}\ h$ at 1.5 mm and a decline to a negligible rate by 3 mm (15). By contrast, rate of incorporation of D-glucose into cellulose is shown to have a broad peak around

3 mm and to decrease slowly with distance, at least as far as 7.5 mm (11). Dry weight deposition follows an intermediate course: it peaks just after 2 mm (where it is 35 $\mu g\ mm^{-1}\ h^{-1}$), drops to 7 $\mu g\ mm^{-1}\ h^{-1}$ at 4.5 mm, rises again to a second peak (approaching 20 $\mu g\ mm^{-1}\ h^{-1}$) at 6 mm, and finally drops to near zero at 8 mm (6). These results accord with the qualitative hypothesis that cell division and protein deposition in the root are coordinated process which cease by 3 mm, while growth (strain) continues with accompanying carbohydrate and wall production processes until a cell reaches a point 10 mm from the tip. Thereafter, differentiation continues in the absence of strain; and it is probable that metabolic turnover is high (3) even in the observed absence of net metabolite deposition.

Acknowledgments—We thank A. Matista for skillful technical assistance. This paper was written while the senior author was spending a sabbatical in the labortory of Professor E. Miginiac, Universite de Paris and CNRS Service Phytotron, Gif-sur-Yvette.

LITERATURE CITED

1. AHMED AER, JM LABAVITCH 1978 A simplified method for accurate determination of cel wall uronide content. J Food Biochem 1: 361–365
2. ERICKSON RO 1976 Modeling of plant growth. Annu Rev Plant Physiol 27: 407–434
3. ERICKSON RO, DR GOODARD 1951 An analysis of root growth in cellular and biochemical terms. Growth Symp 10: 89–116
4. ERICKSON RO, KB SAX 1956 Elemental growth root of the primary root of *Zea mays*. Proc Am Philos Soc 100: 487–498
5. ERICKSON RO, MWK SILK 1980 The kinematics of plant growth. Sci Am 242: 134–151
6. GANDAR PW 1980 The analysis of growth and cell production in root apices. Bot Gaz 141: 131–138
7. GANDAR PW 1983 Growth in root apices. I. The kinematic description of growth. II. Deformation and rate of deformation. Bot Gaz 144: 1–10, 11–19
8. GREEN PB 1976 Growth and cell pattern formation on an axis: Critique of concepts, terminology and modes of study. Bot Gaz 137: 187–202
9. NISHITANI K, Y MASUDA 1979 Growth and cell wall changes in azuki bean epicotyls. I. Changes in cell wall polysaccharides during intact growth. Plant Cell Physiol 20: 63–74
10. ROBERTS RM 1967 The incorporation of ^{14}C-labeled-D-glucuronate and D-galactose into segments of the root-tip of corn. Phytochemistry 6: 525–533
11. ROBERTS RM, VS BUTT 1967 Patterns of cellulose synthesis in maize root-tips. Exp Cell Res 46: 495–510
12. ROBERTS RM, VS BUTT 1968 Patterns of pentose and uronic acid incorporation into the cell walls of maize root-tips. Exp Cell Res 51: 519–530
13. SILK MWK 1983 Kinematic analysis of leaf expansion. *In* J Dale, ed. The Growth of Leaves. Cambridge University Press, New York, pp 89–108
14. SILK MWK, RO ERICKSON 1979 Kinematics of plant growth. J Theor Biol 76: 481–501
15. SILK MWK, RO ERICKSON 1980 Protein deposition rates in the growing corn root. J Theor Biol 83: 701–703
16. VAN HOLST GJ, FM KLIS, F BOUMAN, D STEGWEE 1980 Changing cell wall compositions in hypocotyls of dark-grown bean seedlings. Planta (Berl) 149: 209–212

APPENDIX

Utility of the one-dimensional continuity equation for radially symmetrical tissues.

Assumptions:

1. Radial strain rate is uniform in the plane of the cross-section, therefore

$$\nabla \cdot v = \frac{\partial v_z}{\partial z} + \frac{2v_r}{r} = \frac{\partial v_z}{\partial z} + \frac{2}{r}\frac{\partial r}{\partial z} v_z$$

2. In the cross-section, average deposition rate is of interest; and average density, $\bar{\rho}$, can be studied

$$\bar{\rho} = \frac{1}{\pi r^2}\int_A \rho dA \Rightarrow \frac{\partial \bar{\rho}}{\partial r} = 0$$

Then a two-dimensional treatment gives

$$D = \frac{\partial \bar{\rho}}{\partial t} + \frac{\partial \bar{\rho}}{\partial z} v_z + \bar{\rho}\left(\frac{\partial v_z}{\partial z} + \frac{2}{r}\frac{\partial r}{\partial z} v_z\right) \quad \text{(A1)}$$

In the one-dimensional experiment, we measure the amount of substance in the cross-sectional slices, $\bar{\rho}\pi r^2$, to obtain an apparent deposition rate, D'

$$D' = \frac{\partial}{\partial t}\left(\bar{\rho}\pi r^2\right) + \frac{\partial}{\partial z}\left(\bar{\rho}\pi r^2\right)v_z + \left(\bar{\rho}\pi r^2\right)\left(\frac{\partial v_z}{\partial z}\right) \quad \text{(A2)}$$

Expanding the middle term and dividing by πr^2 gives

$$\frac{D'}{\pi r^2} = \frac{\partial \bar{\rho}}{\partial t} + \frac{\partial \bar{\rho}}{\partial z} v_z + \bar{\rho}\left(\frac{2}{r}\frac{\partial r}{\partial z} v_z + \frac{\partial v_z}{\partial z}\right) \quad \text{(A3)}$$

Therefore

$$\frac{D'}{\pi r^2} = D \quad \text{(A4)}$$

This implies that the deposition rate per unit length, given by A2, can be divided by the local cross-sectional area to obtain the local deposition rate per unit tissue volume.